The Impact of Seamount Topography on Ocean Currents in the Western Tropical Pacific Ocean

Caitlyn McCulloch

University Of Washington

School of Oceanography

caitmcc@uw.edu

06/05/2026

Abstract

This study integrates physical oceanography and marine geology to survey seamounts in the Western Tropical Pacific Ocean near Guam. Seamounts are significant because of their ability to manipulate ocean currents and wave turbulence on both a local and global scale. Seamounts within this region are abundant due to their location on a subduction zone along the Mariana Arc, but there is limited data identifying how their structures influence the regional currents in this area. The objective of this study is to determine the relationship between the slope of a seamount and the surrounding current velocities. I hypothesized that horizontal currents would be faster around seamounts with steeper topographic slopes compared to seamounts with flatter slopes. To analyze fluid flow interactions with seamount topography, this study measured current velocities with an Acoustic Doppler Current Profiler and imaged seafloor bathymetry using multibeam sonar techniques around two seamounts near the Mariana Arc, named NW Rota-1 and Ruby. I found that current speeds around North West Rota-1 were faster than at the other seamount Ruby, but I did not observe a clear relationship between topographic slope and current speed. Although these results suggest that shallower seamounts are associated with stronger flows than deeper seamounts, more observations are needed to understand the impact of seamount slope on the surrounding oceanographic currents.

Plain Language Summary

In the Western Tropical Pacific Ocean, there is a unique abundance of underwater mountains called seamounts, created by the volcanic Mariana Arc. Seamounts are underwater mountains that can be dormant or active volcanoes. The purpose of this study was to understand how currents in the surrounding waters are affected by the presence of these seamount structures. I hypothesized that seamounts with steeper slopes would have faster currents in the surrounding waters. I believe the cone structure would create a steeper slope, which makes a runway for the water to speed up, creating more water flow. To examine this, I measured water velocities in the upper ocean, along a north-south and an east-west transect across two seamounts near the Mariana Arc, while also mapping the seafloor using multibeam sonar technology. The data revealed that current speeds were faster around the shallower, steeper seamount compared the deeper, less steep seamount. The findings in this study provide evidence of a relationship between seamount depth and the strength of the surrounding currents, which can hopefully motivate future studies on seamounts and their influence on enhancing mixing and transport of nutrients.

Introduction

Seamounts are a common geologic feature found underwater, forming as a byproduct of rising magma that pierces through the ocean floor. In response to subducting tectonic plates, seamounts typically exist along volcanic arcs as active submarine volcanoes themselves (Baker et al., 2008). The size and depth ranges of seamounts vary, with some found as deep as the twilight zone (200 meters - 1000 meters) and others as shallow as the euphotic zone (< 200 m) (Wang *et al.,* 2024). The exact population of seamounts is still unknown, but hydrodynamic studies have shown that the presence of a seamount can create obstacles for ocean currents, thereby altering fluid flow that differs from open ocean currents (Turnewitsch et al., 2013).

Oligotrophic oceans are areas of ocean water where primary productivity is low, leading to the low nutrients and export of other organic matter (Wang et al., 2024). Seamounts are typically found in these areas and function as an ecological oases due to the abundance of nutrients being upwelled, providing habitats for fish and food for microbial communities (Lavelle et al., 2020). Without the presence of these seamounts, many oligotrophic areas of the ocean would lack mixing and productivity driven by the associated upwelled nutrients. Examining the interactions between seamounts and oceanic currents thus helps us to understand the chemical, biological and sedimentological changes associated with seamounts.

Above a seamount, researchers have found the presence of a Taylor Cap, where a stationary vortex rotates above the seamount creating an isolated region of flow (Lavelle et al., 2020). This process, which only occurs with weak fluid flow, entraps water above the seamount while also retaining and redistributing sediments throughout the surrounding water column (Liu et al., 2023). For stronger fluid flow, seamounts manipulate currents through the generation of lee waves, which are created with strong currents traveling over rough topographic features on the seafloor. As lee waves propagate away from the seamount summit and break, turbulent mixing occurs at the bottom of the sea floor and creates enhanced mixing near the seabed (Zheng et al., 2024). Thus, seamount generated mixing from lee waves contributes to the upwelling of deep ocean water in various areas of the world.

To determine how impactful seamounts are on oceanic current flow, this study focuses on the Western Topical Pacific Ocean, a unique area where the average surface seawater temperature is 28 °C (Ma et al., 2023). Compared to the average global ocean temperature at 17 °C, the Western Tropical Pacific has the warmest ocean surface water in the world (University of Hawaiʻi at Mānoa, n.d.). These warmer waters are more susceptible to ocean stratification due to a lack of upwelling and mixing, and in many cases can be characterized as an oligotrophic ocean. In addition to the high sea temperatures, seamounts along the Izu-Bonin Mariana Arc are predominately a submarine intraoceanic arc, meaning it's bordered on oceanic crust on both sides and one plate is subducting under the other (Baker et al., 2008). Within this region, seamounts have tall slopes with caldera or cone peak classifications, resulting in varying current speeds and directional variability (Baker et al., 2008). There are over 60 submarine volcanoes in the Mariana Arc, but this study examines two cone seamounts, North West Rota-1 seamount and Ruby seamount (Schnur, et al. (2017)). In a 2008 study by *Baker et al.,* NW Rota 1 was classified to have a cone shape, meaning steep topography with a cone shaped summit. Since then, another study on NW Rota-1's bathymetry in 2017 revealed the summit had experienced changes from landslides caused by collapsing vents, plumes, and other erupting activity (Schnur, et al., 2017).

Although individual seamounts such as NW Rota-1 have been studied extensively due to their active volcanism and evolving topography, the unique characteristics of these sites may not represent all seamount systems. Less-documented seamouts, such as Ruby, therefore require further investigation to determine whether similar hydrodynamic and bathymetic processes occur across different seamount structures. For this study, I hypothesized that horizontal current speeds will be faster around seamounts with steeper topographic slopes compared to seamounts with flatter slopes, which will have less intense current speeds. I predicted this outcome because I believe that steeper slopes on a seamount will further disrupt current flow compared to a seamount with a flatter slope. Seamounts are known to modify surrounding ocean circulation through topographic steering, eddy interactions, and enhance mixing processes (Hanafi-Portier et al., 2024). Previous studies have shown that steep seafloor gradients can intensify near-bottom currents by constricting and redirecting slowly around seamount flanks (Ueno et al., 2024). Based on these findings, this study aims to find answers from these seamount regions with steeper bottom slopes that would have higher current speeds than regions with flatter slopes. We know that seamounts have an influence on current flow, but they are structurally unique and are often located in remote regions of the ocean. Further research on seamount bathymetry can improve our understanding of how fluid dynamics around these features vary, influencing the deep water upwelling and local circulation. This study investigates how variations in two different seamount's shape, height, depth, and slope influence ocean current speeds along the Mariana Arc in the Western Tropical Pacific Ocean.

Methods

Seamount Selection

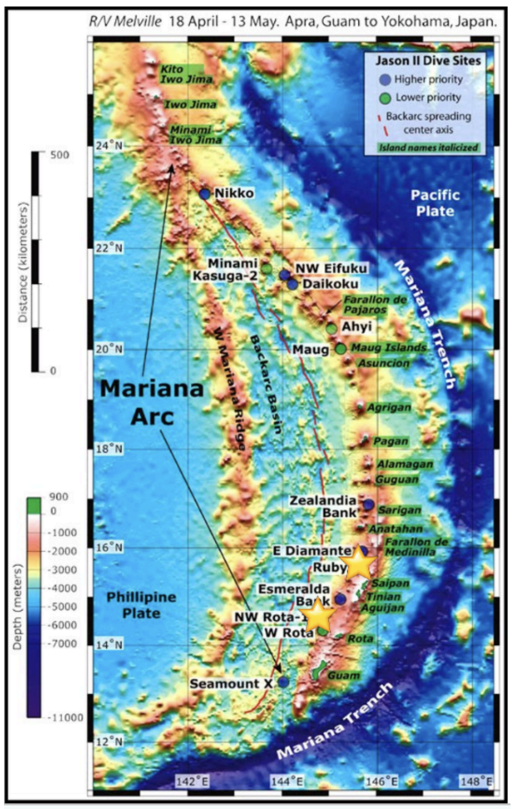

Figure 1. Map of the Mariana Arc, including various seamounts in the region courtesy of the Submarine Ring of Fire 2006 Expedition, NOAA Vents Program. The starred seamounts, NW Rota-1 and Ruby Seamount, are the seamounts used for this study.

There are two active seamounts at somewhat shallow depths that were chosen for this research. NW Rota-1 is located at 14.60° N, 144.78° E around 517 meters below sea level (Figure 1). The second seamount studied is Ruby Seamount, located at 15.62° N, 145.57° E at a depth of around 230 meters (Figure 1). Both of these seamounts were chosen to compare their differences in slope, examined in correlation to the horizontal current strength. Multibeam imaging from a former study gives us a relative idea of the shape, depth, and size of each seamount (Schnur, et al., 2017). However, this imaging is from a study done in 2008, and so it was expected that the bathymetry of the seamounts had changed relative to this previous study.

Multibeam Sonar Imaging

Each seamount aboard the R/V Thompson was mapped using the hull installed Kongsberg EM124 Multibeam system. For sampling, the ship traveled at a speed of 4-5 nautical miles per hour, taking a total of about 9 hours traveling for each seamount. The ship traveled in a bowtie-like path to encompass precise samples of each seamount and ensure high resolution from the beam transmission.

The imagery of each seamount provided from the multibeam sonar mapping is taken from the ship, then processed using Qimera, where any outliers in the beam transmission were cleaned and filtered to produce a proper map. In QGIS, I took the geospatial data and created a bathymetric model of Ruby seamount. NW Rota 1 was mapped and cleaned by Logan Harris, another student working with NW Rota 1. He also analyzed and produced the same results for this seamount using Qimera and QGIS. The results from these models will provide a high resolution visualization of the seamounts slope, shape, and volume.

The slopes of each seamount are made through QGIS where I took the depth of each point and divided it by the distance to the next point. In my analysis, one of my final figures plots the slope against the current speeds at the fastest point in the water column. The x-axis has a negative slope where the ship begins traveling along the transect and becomes more positive towards the end so readers could visualize the seamount both before and after the seamount summit, where the slope is 0 meters per meter.

ADCP Data Collection and Analysis

Velocity data in the upper ocean was collected using a 75kHz Ocean Surveyor Broadband acoustic doppler current profiler (ADCP) from Teledyne RD Instruments. This hull-mounted instrument was set up with a configuration developed and administered by the University of Hawaii's ADCP data collection group for UNOLS vessels. Currents were automatically processed into eastward and northward components by rotating the flow measured relative to the ship into geographic coordinates and removing the ship speed estimated from GPS navigation.

For ADCP data collection, we took multiple points along each transect, each point reaching as deep as 700 meters or less if a shallower bottom was present. For data analysis, this study has two different metrics of bathymetry and current velocity data to filter, plot, and display. ADCP data was uploaded into Python to organize and plot into a visual representation with the current velocities at different depths. I calculated the actual current speeds by squaring the zonal and meridional velocity components, adding them together and then taking the square root of that solution.

$$S = \sqrt{u^2 + v^2}$$

Equation for calculating current speeds.

Once again, north-south and east-west transects were created for each seamount with labeled waypoints after the ship had collected all data. I spaced each point out by about 0.1 degree of latitude or longitude to ensure consistency for slope calculation across both seamounts. I eliminated the surface currents within my data, as these currents might be faster at the surface and I only want to investigate the currents around and about 100 meters above. To do this I only focused on the ADCP data 100 meters above the seamount's summit and below to the maximum instrument depth.

Results

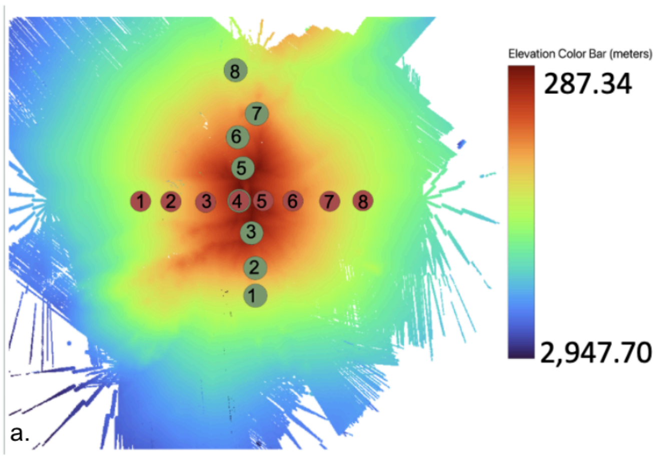

Table 1. Ruby Seamount North-South Transect Points

b.

Point	Latitude (Degrees)	Longitude (Degrees)
1	15.571786	145.575639
2	15.580208	145.575533
3	15.590875	145.574294
4	15.600664	145.570319
5	15.610647	145.571439
6	15.620033	145.569739
7	15.627233	145.575664
8	15.640469	145.568914

Table 2. Ruby Seamount West-East Transect Points

c.

Point	Latitude (Degrees)	Longitude (Degrees)
1	15.600311	144.539306
2	15.600286	144.548861
3	15.600156	145.559758
4	15.600664	145.570319
5	15.600742	145.577903
6	15.600717	145.587217
7	15.600706	145.598792
8	15.600956	145.609222

Figure 2. (a) Birds-eye elevation map of Ruby Seamount, where red is the shallowest and blue is the deepest. ADCP data points are layered on top in a North-South and East-West transect line. The table, Figure 2b and 2c provides the exact latitude and longitude of each labeled point for reference.

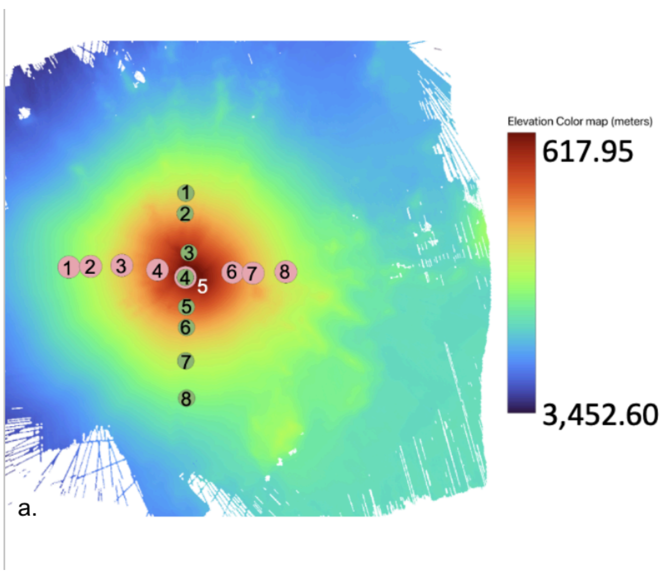

Table 3. NW Rota 1 Seamount North-South Transect Points

b.

Point	Latitude (Degrees)	Longitude (Degrees)
1	14.629181	144.772519
2	14.622147	144.772394
3	14.608608	144.773825
4	14.600058	144.772703
5	14.589836	144.773136
6	14.582764	144.773236
7	14.571208	144.773072
8	14.558306	144.773531

c.

Table 4. NW Rota 1 Seamount West-East Transect Points

Point	Latitude (Degrees)	Longitude (Degrees)
1	14.602317	144.808319
2	14.601764	144.79670
3	14.601931	144.789422
4	14.600058	144.772703
5	14.602592	144.762725
6	14.604006	144.750081
7	14.603542	144.739025
8	14.603228	144.731339

Figure 3. (a) Birds-eye elevation map of NW Rota 1 Seamount, created by UW Senior Thesis student Logan Harris, where red is the shallowest and blue is the deepest. ADCP data points are layered on top in

a North-South and East-West transect line. The table, Figure 3b and 3c provides the exact latitude and longitude of each labeled point for reference.

The multibeam sonar imaging data reveal differences in seamount summit depth and seamount height in meters (Figure 2a and 3a). Ruby seamount has a summit at 287 meters, and a total height of 2,660 meters(Figure 2a). NW Rota 1 has a deeper summit at 617 meters, and a total height of 2,835 meters(Figure 3a). This makes NW Rota larger in height, but deeper in the ocean.

When we examine these transects further with ADCP data, we can see that the faster current speeds are found around Ruby seamount, with some areas as fast as 1 meter per second compared to Rota's fastest speeds around 0.6 m/s (Figure 4 and 5). These faster currents are seen at Ruby before and after the summit, as the white dots exhibit the fastest current speeds throughout the water column bin(Figure 5). NW Rota 1 has no currents faster than 0.6 meters per second, with the white dots here are below and above but still before and after the summit(Figure 6).

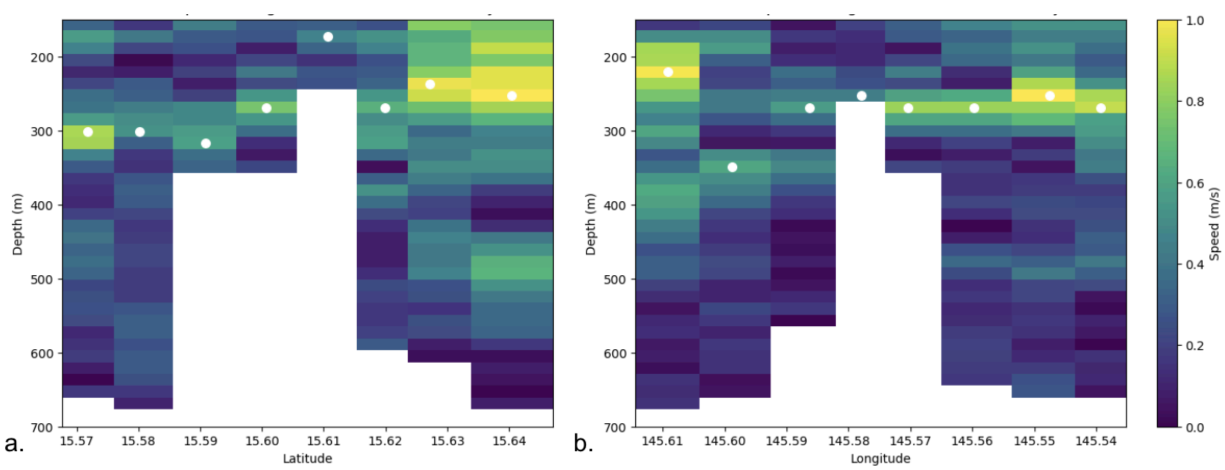

Figure 4. From the previous points, current speeds for Ruby Seamount are calculated and graphed across the North-South (a) and East-West (b) transects. The contour plot has yellow being the fastest speed and dark blue being the slowest speed in meters per second. The white dot

represents the fastest speed within the water column at that point for both Figure 4a and 4b.

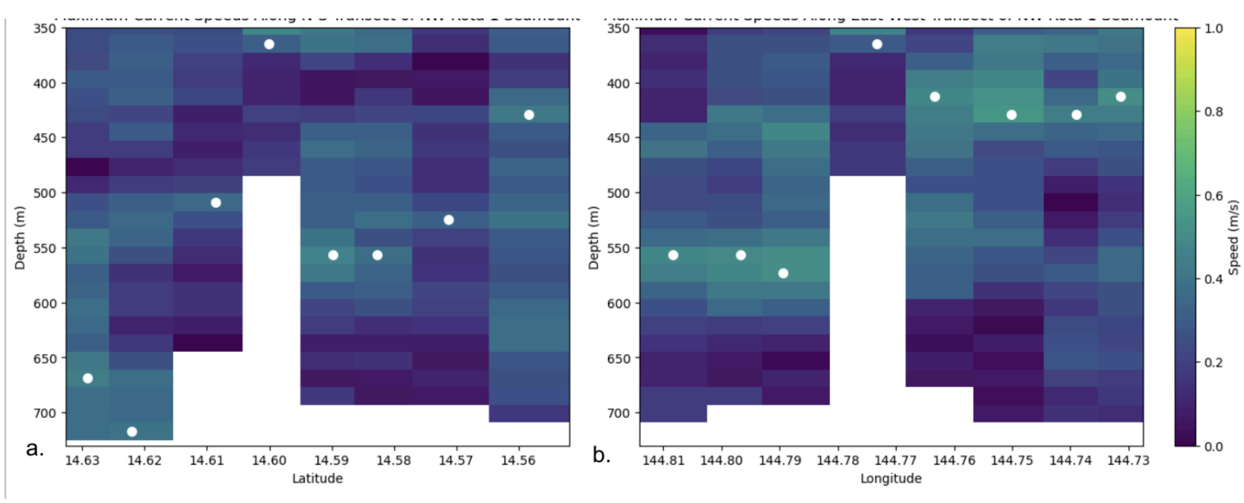

Figure 5. From the previous points, current speeds for NW Rota 1 Seamount are calculated and graphed across the North-South (a) and East-West (b) transects. The contour plot has yellow being the fastest speed and dark blue being the slowest speed in meters per second. The white dot represents the fastest speed within the water column at that point for both Figure 5a and 5b.

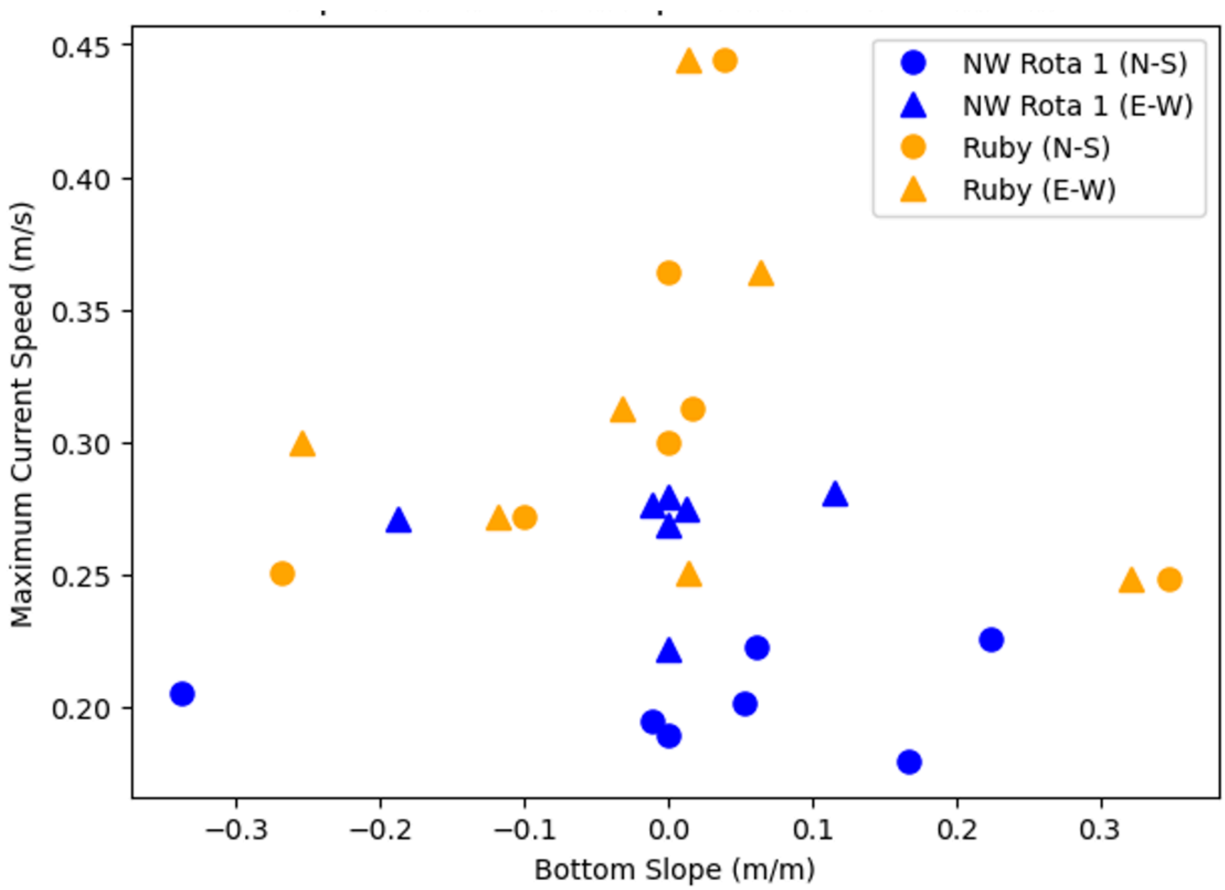

Figure 6. Both seamounts are plotted for their slope and current speeds. The orange is for Ruby, and the Blue is for NW Rota 1, with the different shapes representing the different transects.

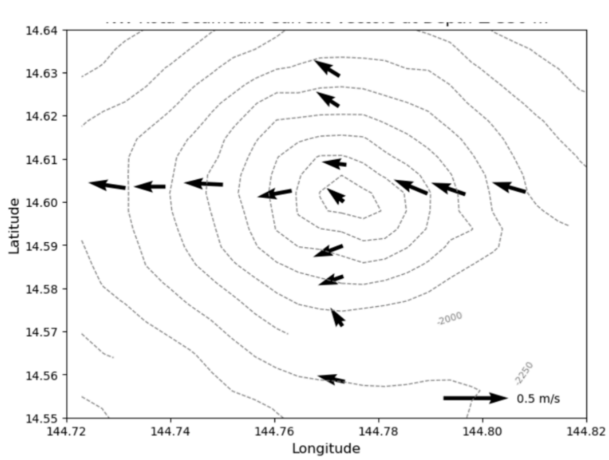

a

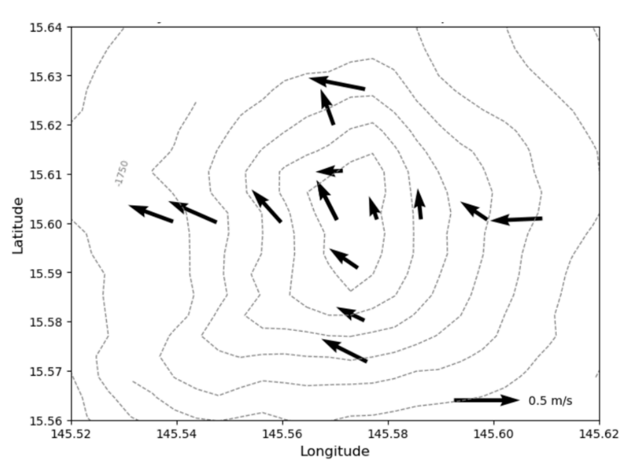

b

Figure 7. NW Rota 1 transects on the left(a), and Ruby seamount transects on the right(b). Arrows represent the directions of currents with speed displayed through the size of each arrow. Gray dotted lines are the contour lines for each seamount plotted from with GebCo.

In the water column, the fastest current speeds are below the summit in the north part of the transect, and above the summit as the transect moves south (Figure 4a). For the East-West transect, the faster currents before crossing the summit are actually at the surface rather than below the summit. Just west of the summit, the current speeds moving West just above Ruby summit are the fastest (Figure 4b). For NW Rota 1, the current speeds do not exhibit any unusual behavior for the downstream transect (Figure 5a). For the East-West transect, there are a few points before the summit where currents get faster closer to the surface, but after passing over the summit the fastest speeds remain at the same depth. At NW Rota 1, current vectors showed greater directional variability around the transect region, whereas Ruby exhibited more coherent westward-directed flow along most of the transect. Ruby also displayed generally larger vector magnitudes, consistent with the higher maximum current speeds observed in other plots (Figure 4, 5, and 6).

After comparing the slope and the current speeds at these seamounts, I found that the slope doesn't have much of a relationship with the maximum speed at NW Rota 1 (Figure 6). At Ruby, however, there is more variability in the maximum speeds, and the fastest currents occur where the slope is near or at zero which is the summit or near the bed. Ruby’s maximum current speeds ranged from 0.25-0.45 m/s, whereas Rota values remained lower, between 0.18-0.28 m/s (Figure 6). Both seamounts had smaller slopes than expected, ranging from 0 to 0.3 meters, with most values classified between 0 m to 0.2 m. Keep in mind that for NW Rota 1, we could only survey the upper 200 meters of this seamount due to ADCP limitations.

Vector plots of near-bottom currents revealed differing flow patterns between the two seamounts (Figure 7). The points plotted along each transect exhibit a uniform current flow around Ruby Seamount, flowing in the north west direction (Figure 7a and 7b). Along the downstream transect, current speeds are faster south of Ruby's summit. Despite higher velocities observed at Ruby seamount, no strong linear relationship between bottom slope and current speed was apparent for either seamount. NW Rota 1 shows little variation in current speed across a range of bottom slopes, while Ruby displays more variability with its slope.

Discussion

The original hypothesis predicted that steeper bottom slopes would correspond to higher current speeds due to the topographic acceleration of flow along seamount flanks. While Ruby exhibited higher current speeds than NW Rota 1, the final scatter plots did not show a strong, direct relationship between slope magnitude and current speed.

At NW Rota 1, current speeds remained somewhat consistent despite variation in bottom slope, suggesting that seamount's slope may not have dominant control on current flow in this region. In contrast, Ruby displayed higher current speeds, indicating that additional oceanographic processes may influence circulation patterns there. Previous studies have shown that circulation around seamounts is often influenced by complex interactions among bathymetry, eddies, regional flow, and internal wave dynamics rather than just slope. Research on abyssal seamounts in the Pacific Northwest demonstrated that surface eddies interacting with seamounts can generate enhanced near-bottom circulation and turbulent mixing. Their results showed that seamounts produced strong localized currents entirely independent of slope gradients (Hanafi-Portier et al., 2024). Additionally, the vector plots in my study also suggest that the seamounts do influence typically steady current flow structures and regional circulation patterns. Similarly, observational studies of deep currents around seamounts have identified highly variable circulation patterns and topographically controlled current flows that differ between seamount systems (Ueno et al., 2024). These findings are consistent with the vector plots generated in this study, which showed higher-magnitude current flow patterns around Ruby compared to NW Rota 1.

The behavior of horizontal current speeds exhibited at Ruby seamount in Figure 4 initially led me to believe there is a lee wave generated from this seamount. However, we would need to look at not only the current speed, but the dissipation rate, Froude number, and or the diapycnal diffusivity to confirm this process (Wang *et al.,* 2024). A lee wave creates enhanced mixing within the deep layer which can improve nutrient availability for organisms in shallower water. We can't confirm that this process is happening at Ruby, but data analysis on the CTD casts from other projects could tell us if upwelling is occurring on the downstream side where current speeds were faster. Typical lee wave characteristics show enhanced mixing on the downstream slope from topographic interference (Wang *et al.,* 2024).

The lack of strong point-by-point relationships between slope and current speed suggests that slope alone is insufficient to explain variability in near-bottom currents. Instead, broader circulation dynamics and seamount bathymetry need to be further investigated to determine consistent flow behavior and which processes identified in previous studies are occurring.

Conclusions

Deep ocean currents in the Western Tropical Pacific are strongly influenced by seamount topography. However, the specific fluid dynamic processes controlling circulation around seamounts likely vary depending on factors such as seamount size, shape, summit depth, and regional circulation patterns. Future research should further investigate whether these circulation patterns are consistent across shallow seamount systems such as Ruby seamount, which has a summit depth of approximately 200 meters. Additional observations are also needed at NW Rota 1, where the ADCP measurements were limited to approximately 700 meters below the surface despite the seamount extending to depths near 3000 meters. Expanding observations deeper the the seabed floor around seamounts would improve understanding of summit to seafloor current interactions. As additional datasets from the University of Washington Senior Thesis cruise become available, future studies could also examine relationships among current flow, nutrient concentrations, chlorophyll, and plankton productivity. The investigation of this topic helps support previous studies emphasizing the ecological importance of these seamounts and their unique oceanographic systems.

Acknowledgements

I would like to acknowledge the University of Washington School of Oceanography for the senior thesis cruise. Additionally I would like to thank the captain and crew of the R/V Thomas G. Thompson. Lastly, I would like to thank my mentor Alison Gray for all of her support.

References

Baker, E. T., R. W.Embley, S. L.Walker, J. A.Resing, J. E.Lupton, K.-I.Nakamura, C. E. J.de Ronde, and G. J.Massoth (2008), Hydrothermal activity and volcano distribution along the Mariana arc, J. Geophys. Res., 113, B08S09, doi:10.1029/2007JB005423.

Hanafi-Portier, M., S. Samadi, L. Corbari, M. Boulard, E. Miramontes, P. Penven, B. Leroy, T. Napoléon, S. J. Jorry, and K. Olu (2024), Multiscale spatial patterns and environmental drivers of seamount and island slope megafaunal assemblages along the Mozambique Channel, *Deep Sea Research Part I: Oceanographic Research Papers*, **203**, 104198, https://doi.org/10.1016/j.dsr.2023.104198.

Lavelle, J. W., and C. Mohn (2010), Motion, commotion, and biophysical connections at deep ocean seamounts, *Oceanography*, 23(1), 90–103, https://doi.org/10.5670/oceanog.2010.64.

Liu, Y., Q. Ren, F. Yu, et al. (2023), Observed Taylor cap around a seamount intensified by a surface mesoscale eddy in the Northwest Pacific, *Climate Dynamics*, 61, 849–859, https://doi.org/10.1007/s00382-022-06570-0.

Ma, J., X. Li, J. Song, Q. Wang, L. Wen, K. Xu, G. Zhong, J. Dai, J. Xing, and D. Tian (2023), Relationship and stratification of multiple marine ecological indicators: A case study in the M2 seamount area of the Western Pacific Ocean, *Ecological Indicators*, 146, 109804, https://doi.org/10.1016/j.ecolind.2022.109804

Mohn, C., A. Denda, S. Christiansen, M. Kaufmann, F. Peine, B. Springer, R. Turnewitsch, and B. Christiansen (2018), Ocean currents and acoustic backscatter data from shipboard ADCP measurements at three North Atlantic seamounts between 2004 and 2015, *Data in Brief*, 17, 237–245, https://doi.org/10.1016/j.dib.2018.01.014

Schnur, S. R., et al. (2017), A decade of volcanic construction and destruction at the summit of NW Rota-1 seamount: 2004–2014, *Journal of Geophysical Research: Solid Earth*, 122, 1558–1584, https://doi.org/10.1002/2016JB013742

Turnewitsch, R., S. Falahat, J. Nycander, A. Dale, R. B. Scott, and D. Furnival (2013), Deep-sea fluid and sediment dynamics—Influence of hill- to seamount-scale seafloor topography, *Earth-Science Reviews*, 127, 203–241, https://doi.org/10.1016/j.earscirev.2013.10.005

Ueno, T., Fujio, S. & Yanagimoto, D. Observation of deep currents around a seamount between the Japan and Kuril trenches. *J Oceanogr* 80, 365–374 (2024). https://doi.org/10.1007/s10872-024-00732-w

Wang, X., et al. (2024), Seamounts generate efficient active transport loops to nourish the twilight ecosystem, *Science Advances*, 10, eadk6833, https://doi.org/10.1126/sciadv.adk6833

Zheng, K., Zhang, Z., Yang, Z., Sun, H., Guan, S., Huang, X., et al. (2024). Influence of lee wave breaking on far-field mixing in the deep ocean. Journal of Geophysical Research: Oceans, 129, e2023JC020386. https://doi.org/10.1029/2023JC020386